Journal of Organometallic Chemistry, 310 (1986) 55–65
Elsevier Sequoia S.A., Lausanne – Printed in The Netherlands

CRYSTAL STRUCTURE OF $[Ph_4As]_2[Re_7C(CO)_{21}Au(PPh_3)]$. COMPARISON OF H^+ AND $Au(PPh_3)^+$ COORDINATION TO $[Re_7C(CO)_{21}]^{3-}$

TIMOTHY J. HENLY, JOHN R. SHAPLEY*

School of Chemical Sciences and Materials Research Laboratory, University of Illinois, Urbana, Illinois 61801 (U.S.A.)

and ARNOLD L. RHEINGOLD*

Department of Chemistry, University of Delaware, Newark, Delaware 19711 (U.S.A.)

(Received February 11th, 1986)

Summary

The structure of $[Ph_4As]_2[Re_7C(CO)_{21}Au(PPh_3)]$ has been determined by X-ray crystallography. The mixed-metal cluster anion adopts a 1,4- (i.e. *trans*-) bicapped octahedral geometry. Solution ^{13}C NMR spectra reveal that this $Au(PPh_3)^+$ adduct of $[Re_7C(CO)_{21}]^{3-}$ maintains the (1,4)-bicapped structure in solution whereas the corresponding H^+ adduct, $[HRe_7C(CO)_{21}]^{2-}$, displays two isomers.

Introduction

A series of high-nuclearity rhenium carbido clusters (composed of $[H_2Re_6C(CO)_{18}]^{2-}$, $[Re_7C(CO)_{21}]^{3-}$, and $[Re_8C(CO)_{24}]^{2-}$) has been reported by Ciani et al. [1–3]. These compounds can be viewed as having a common $[Re_6C(CO)_{18}]^{4-}$ octahedral core with either H^+ or $Re(CO)_3{}^+$ moieties capping triangular faces. The crystal structure of $[Re_8C(CO)_{24}]^{2-}$ [3] shows the capped faces to be (1,4)-related, whereas crystallographic and variable-temperature ^{13}C NMR studies of $[H_2Re_6C(CO)_{18}]^{2-}$ [1] suggest that the hydrogen atoms cap adjacent (1,2)-trirhenium faces (see Scheme 1 for nomenclature).

Independent work in our laboratory has resulted in the facile synthesis of $[Re_7C(CO)_{21}]^{3-}$ from $Re_2(CO)_{10}$ [4], and we were interested in whether the reactions of this cluster with electrophiles would lead to adducts with structures analogous to that of $[Re_8C(CO)_{24}]^{2-}$ or $[H_2Re_6C(CO)_{18}]^{2-}$. The recent report by Beringhelli et al. on the reactions of $[Re_7C(CO)_{21}]^{3-}$ with copper triad electrophiles [5] prompts us to report some aspects of our work. Specifically, we have obtained the crystal structure of $[Re_7C(CO)_{21}Au(PPh_3)]^{2-}$, which has been reported but not structurally characterized [5]. We have also investigated the solution structure of this

0022-328X/86/$03.50

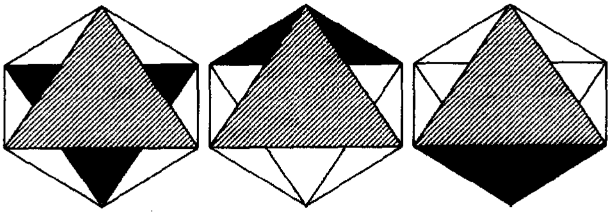

(1,4) (1,3) (1,2)

SCHEME 1. Shaded areas represent capped faces.

compound in comparison with its hydride analogue, $[HRe_7C(CO)_{21}]^{2-}$, by variable-temperature ^{13}C NMR spectroscopy.

Results and discussion

Et_4N^+, Ph_4As^+, and PPN^+ ($PPN^+ = (Ph_3P)_2N^+$) salts of $[Re_7C(CO)_{21}Au(PPh_3)]^{2-}$ were prepared by treatment of the corresponding salt of $[Re_7C(CO)_{21}]^{3-}$ with $Au(PPh_3)Cl$ in refluxing nitromethane; the PPN^+ product was characterized by infrared spectroscopy, elemental analysis, and fast-atom bombardment mass spectroscopy (FAB-MS). Diffraction-quality crystals of the tetraphenylarsonium salt were obtained from acetone/isopropanol.

The solid-state structure of $[Re_7C(CO)_{21}Au(PPh_3)]^{2-}$ is shown in Fig. 1. (Tables 1 and 2 contain selected bonding parameters and atomic coordinates, respectively.) The $(Ph_3P)Au$ moiety triply bridges the trirhenium face *trans* to the unique $Re(CO)_3$, resulting in a (1,4)-bicapped octahedral structure (of idealized C_{3v} symmetry) analogous to that of $[Re_8C(CO)_{24}]^{2-}$ [3]. The variation in the rhenium–rhenium bond distances (2.96–3.08 Å, with the longest bonds forming the base of the Au cap) results in a cluster geometry which resembles the monocapped $[Re_7C(CO)_{21}]^{3-}$ more closely than the bicapped $[Re_8C(CO)_{24}]^{2-}$; in this respect the structures of the Re_7Au framework and the Re_7Ag fragments of $[(Re_7C(CO)_{21}Ag)_2(\mu\text{-Br})]^{5-}$ [5] are virtually identical. There is only a slight variation in the rhenium–gold bond distances (2.856–2.893 Å), in contrast to the highly asymmetrical coordination of $Au(PPh_3)$ observed in $Ru_6C(CO)_{15}(NO)(AuPPh_3)$ [6]. The average rhenium–gold bond distance, 2.873 Å, is longer than those observed in other complexes (2.615 Å in $(\eta^5\text{-}C_5H_5)Re(CO)(p\text{-}N_2C_6H_4OMe)(AuPPh_3)$ [7]; 2.805 Å (average) in $[Au_5ReH_4(PPh_3)_7]^{2+}$ [8]). This lengthening may be due to steric interactions of the gold atom with the carbonyl ligands and/or the μ_3 coordination of the $Au(PPh_3)$ moiety in the Re_7Au complex. It is worth noting that a similar effect is observed in $FeCo_3(CO)_{12}(\mu_3\text{-}AuPPh_3)$: the cobalt–gold bond distance in this complex is 0.21 Å longer than that observed in binuclear $Co(CO)_4AuPPh_3$ [9,10]. Finally, the Au–P bond vector in the Re_7Au complex deviates from perpendicularity to the Re(5)–Re(6)–Re(7) plane by about 9°; this may be merely a packing distortion.

The ^{13}C NMR spectrum of $[PPN]_2[Re_7C(CO)_{21}Au(PPh_3)]$ in CD_2Cl_2 at 20°C (Fig. 2) consists of singlets at δ 437.2 (1C, carbide), 206.8 (3C, CO's on Re(1)), 194.2 (9C, CO's on Re(5), Re(6), Re(7)), and 192.3 (9C, CO's on Re(2), Re(3), Re(4)). This pattern is consistent with the solid-state structure, assuming local scrambling of the carbonyls on each rhenium atom [1,3]. As the sample is cooled, the resonances at δ

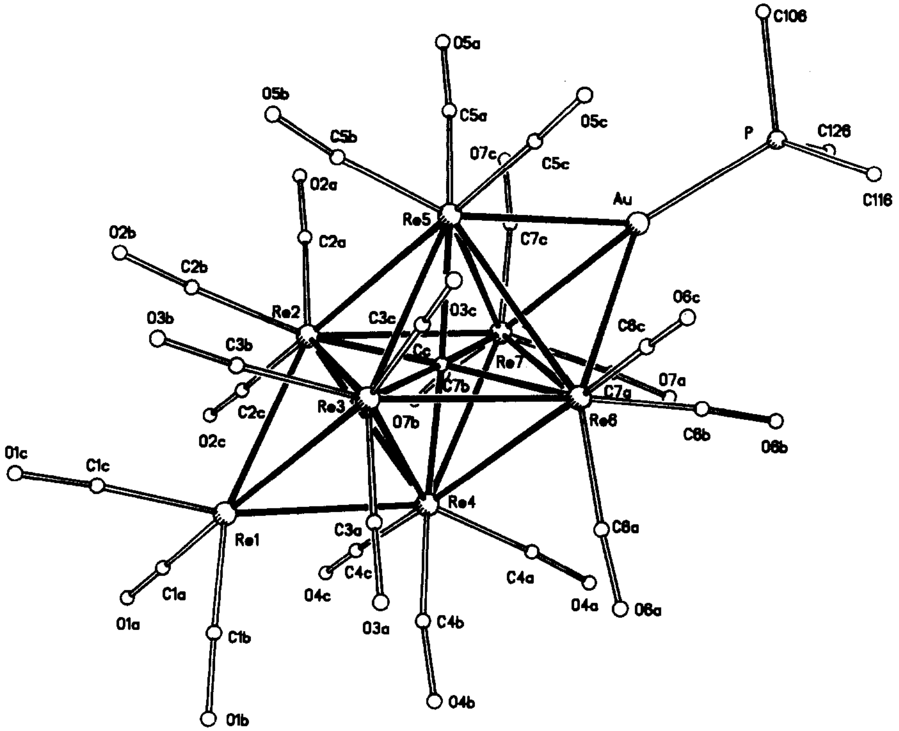

Fig. 1. Solid-state structure of $[Re_7C(CO)_{21}Au(PPh_3)]^{2-}$ (only *ipso*-carbons of phenyl groups shown).

194.2 and 192.3 broaden and split to give a stopped-exchange spectrum at −60°C consisting of four carbonyl resonances: δ 206.7 (3C), 196.5 (6C), 193.1 (6C), and 188.4 (6C). The carbide resonance remains unchanged. These signals can be as-

(Continued on p. 60)

TABLE 1

SELECTED BOND DISTANCES (Å) AND ANGLES (°) FOR $[Ph_4As]_2[Re_7C(CO)_{21}Au(PPh_3)]$

Re(1)–Re(2)	2.968(1)	Re(4)–Re(6)	2.994(1)
Re(1)–Re(3)	2.980(1)	Re(4)–Re(7)	2.992(1)
Re(1)–Re(4)	2.965(1)	Re(5)–Re(6)	3.084(1)
Re(2)–Re(3)	2.961(1)	Re(5)–Re(7)	3.072(1)
Re(2)–Re(4)	2.978(1)	Re(6)–Re(7)	3.078(1)
Re(2)–Re(5)	3.014(1)	Re(5)–Au	2.856(1)
Re(2)–Re(7)	2.998(1)	Re(6)–Au	2.893(1)
Re(3)–Re(4)	2.974(1)	Re(7)–Au	2.869(1)
Re(3)–Re(5)	2.986(1)	Au–P	2.302(5)
Re(3)–Re(6)	3.022(1)	av. Re–$C_{carbide}$	2.13(1)

All angles within 1.0° of those required for a regular octahedron for Re(2) to Re(7) and a regular tetrahedron for the Re(1) cap.

Re(5)–Au–Re(6)	64.9(0)	P–Au–Re(5)	142.0(2)
Re(5)–Au–Re(7)	64.9(0)	P–Au–Re(6)	134.3(1)
Re(6)–Au–Re(7)	64.6(0)	P–Au–Re(7)	147.9(2)

TABLE 2

ATOMIC COORDINATES ($\times 10^4$) AND ISOTROPIC THERMAL PARAMETERS ($Å^2 \times 10^3$)

Atom	x	y	z	U [a]
Re(1)	12128(1)	3324(1)	6292(1)	56(1)*
Re(2)	10972(1)	1842(1)	6970(1)	43(1)*
Re(3)	11632(1)	3469(1)	7504(1)	43(1)*
Re(4)	9838(1)	3693(1)	6911(1)	42(1)*
Re(5)	10478(1)	1985(1)	8196(1)	40(1)*
Re(6)	9302(1)	3899(1)	8126(1)	41(1)*
Re(7)	8637(1)	2194(1)	7573(1)	40(1)*
Au	8241(1)	2375(1)	8737(1)	47(1)*
As(1)	6048(2)	2130(2)	3954(1)	58(1)*
As(2)	3289(2)	2306(2)	2100(1)	51(1)*
P	7040(4)	2252(4)	9569(2)	45(2)*
C(101)	7208(11)	1454(9)	10561(6)	85(8)
C(102)	7578	772	10880	97(9)
C(103)	8242	15	10633	84(8)
C(104)	8536	−60	10065	73(7)
C(105)	8166	622	9746	61(6)
C(106)	7502	1379	9994	48(5)
C(111)	7840(9)	3706(10)	10057(6)	64(6)
C(112)	7757	4537	10348	76(7)
C(113)	6731	4978	10558	74(7)
C(114)	5788	4587	10477	83(8)
C(115)	5871	3755	10187	59(6)
C(116)	6897	3315	9977	48(5)
C(121)	5183(11)	2501(9)	9175(5)	54(6)
C(122)	4083	2423	9169	72(7)
C(123)	3442	1846	9539	88(8)
C(124)	3900	1347	9916	83(8)
C(125)	5000	1425	9922	62(6)
C(126)	5641	2002	9552	52(5)
Cc	10111(13)	2852(11)	7555(8)	37(7)*
C(1a)	12044(20)	3052(18)	5548(10)	80(11)*
O(1a)	12020(17)	2894(15)	5113(7)	116(10)*
C(1b)	12569(16)	4485(16)	6083(10)	66(9)*
O(1b)	12790(15)	5255(11)	5913(7)	89(8)*
C(1c)	13646(21)	2933(19)	6087(9)	91(12)*
O(1c)	14548(15)	2703(14)	5927(9)	116(10)*
C(2a)	10553(16)	608(16)	7088(8)	58(9)*
O(2a)	10324(15)	−192(9)	7156(8)	86(8)*
C(2b)	12466(19)	1354(15)	6852(10)	65(10)*
O(2b)	13357(13)	1026(11)	6795(8)	90(8)*
C(2c)	10921(18)	1519(14)	6238(10)	65(10)*
O(2c)	10800(16)	1264(11)	5815(7)	96(9)*
C(3a)	11978(16)	4712(16)	7344(9)	51(8)*
O(3a)	12181(14)	5487(11)	7258(8)	83(8)*
C(3b)	13160(21)	3070(18)	7300(11)	83(12)*
O(3b)	14092(13)	2835(14)	7226(8)	103(9)*
C(3c)	11967(20)	3661(16)	8217(10)	69(11)*
O(3c)	12234(15)	3817(13)	8630(7)	102(9)*
C(4a)	8348(18)	4201(14)	6996(9)	58(9)*
O(4a)	7496(14)	4514(11)	7014(7)	81(8)*
C(4b)	10302(16)	4881(14)	6713(10)	57(9)*
O(4b)	10417(14)	5678(10)	6608(8)	86(8)*
C(4c)	9787(21)	3349(17)	6179(11)	71(11)*

TABLE 2 (continued)

Atom	x	y	z	U^a
O(4c)	9608(15)	3124(13)	5769(8)	94(9)*
C(5a)	10048(14)	784(14)	8377(9)	57(8)*
O(5a)	9883(13)	−8(9)	8497(6)	68(7)*
C(5b)	19973(16)	1524(14)	8127(8)	51(8)*
O(5b)	12814(13)	1213(12)	8122(7)	80(8)*
C(5c)	10448(16)	2250(14)	8966(9)	54(9)*
O(5c)	10518(13)	2415(12)	9405(7)	74(7)*
C(6a)	9442(19)	5197(19)	7921(9)	77(10)*
O(6a)	9468(17)	5959(11)	7820(8)	102(9)*
C(6b)	7794(16)	4202(14)	8438(8)	48(8)*
O(6b)	6882(13)	4450(10)	8624(7)	72(7)*
C(6c)	9624(21)	4278(16)	8797(11)	81(11)*
O(6c)	9890(16)	4552(12)	9190(8)	102(10)*
C(7a)	7148(17)	2714(14)	7764(9)	58(9)*
O(7a)	6290(13)	2989(11)	7840(7)	67(7)*
C(7b)	8399(19)	1778(16)	6911(11)	71(11)*
O(7b)	8163(15)	1541(13)	6503(8)	94(9)*
C(7c)	8187(16)	1034(15)	7862(11)	81(11)*
O(7c)	7999(13)	258(11)	7982(8)	86(8)*
C(21)	6679(10)	1235(9)	2908(6)	68(7)
C(22)	7355	1059	2393	70(7)
C(23)	8279	1567	2214	84(8)
C(24)	8528	2252	2549	72(7)
C(25)	7852	2428	3064	68(7)
C(26)	6928	1920	3244	53(5)
C(31)	7848(13)	1287(10)	4301(5)	88(8)
C(32)	8609	1162	4625	82(8)
C(33)	8560	1756	5067	75(7)
C(34)	7751	2474	5184	95(9)
C(35)	6989	2599	4860	70(7)
C(36)	7038	2005	4418	62(6)
C(41)	4656(14)	3631(11)	4488(6)	79(7)
C(42)	4093	4496	4511	108(10)
C(43)	4188	5030	4042	99(9)
C(44)	4847	4699	3550	84(8)
C(45)	5409	3834	3526	63(6)
C(46)	5314	3300	3996	73(7)
C(51)	3899(16)	1493(11)	4117(8)	114(11)
C(52)	3134	814	4183	157(15)
C(53)	3456	−108	4258	106(10)
C(54)	4542	−351	4269	115(11)
C(55)	5307	329	4204	103(10)
C(56)	4986	1251	4128	71(7)
C(61)	2556(11)	3043(10)	3168(7)	71(7)
C(62)	1876	3106	3689	91(8)
C(63)	965	2570	3823	88(8)
C(64)	733	1972	3435	79(7)
C(65)	1413	1909	2914	87(8)
C(66)	2324	2444	2780	62(6)
C(71)	1748(12)	1920(9)	1456(6)	75(7)
C(72)	1177	2103	1049	79(7)
C(73)	1409	2871	714	84(8)
C(74)	2213	3456	787	83(8)
C(75)	2785	3273	1194	70(7)

continued

TABLE 2 (continued)

Atom	x	y	z	U^a
C(76)	2552	2505	1529	52(5)
C(81)	5523(12)	2780(7)	1913(6)	66(6)
C(82)	6364	3391	1851	82(8)
C(83)	6115	4343	1914	78(7)
C(84)	5025	4685	2040	78(7)
C(85)	4184	4074	2103	58(6)
C(86)	4433	3122	2039	50(5)
C(91)	4287(12)	641(10)	1549(5)	70(7)
C(92)	4731	−269	1523	96(9)
C(93)	4780	−742	2002	83(8)
C(94)	4385	−304	2506	85(8)
C(95)	3940	606	2532	73(7)
C(96)	3891	1079	2054	46(5)

[a] ★ = Equivalent isotropic U defined as one third of the trace of the orthogonalised U_{ij} tensor.

signed as arising from, respectively: (a) the three carbonyls on the capping Re atom; (b) the six carbonyls pointing toward the $Au(PPh_3)$ cap; (c) the six carbonyls pointing toward the $Re(CO)_3$ cap; (d) the six carbonyls around the "belt" of the octahedron (two accidentally degenerate sets of three).

If $[PPN]_3[Re_7C(CO)_{21}]$ is allowed to react with $HBF_4 \cdot OEt_2$ in dichloromethane at −78°C, a red-brown product is formed immediately. This compound has been characterized by infrared and ^1H NMR spectroscopies, elemental analysis, and FAB-MS as $[PPN]_2[HRe_7C(CO)_{21}]$; it is the only product formed, even in the presence of a large excess of HBF_4. All attempts to grow X-ray quality crystals failed, so we turned to ^{13}C NMR spectroscopy to determine the structure.

The variable-temperature behavior of $[HRe_7C(CO)_{21}]^{2-}$ (Fig. 3) differs significantly from that of $[Re_7C(CO)_{21}Au(PPh_3)]^{2-}$. In CD_3NO_2 at 75°C, the expected fast-exchange pattern is observed: δ 205.4 (3C), 195.3 (9C), and 193.0 (9C). No carbide signals appear. In CD_2Cl_2 at 0°C, five resonances are observed in the carbonyl region (δ 204.2, 196.0, 192.3, 191.7, 190.4) and two in the carbide region (δ 422.3, 415.9). Since this temperature is significantly higher than that required to freeze out local carbonyl scrambling in $[Re_7C(CO)_{21}Au(PPh_3)]^{2-}$, $[H_2Re_6C(CO)_{18}]^{2-}$ [1], $[Re_8C(CO)_{24}]^{2-}$ [3], or $[Re_7C(CO)_{21}]^{3-}$ [11], we believe that hydride motion is involved (see below). At −40°C the signals at δ 196.0 and 190.4 begin to broaden; by −80°C they have split into a pattern of smaller peaks. The signals at δ 192.3 and 191.7 also begin to collapse at −80°C.

This behavior is consistent with the presence of a mixture of isomers in solution (see Fig. 4). The predominant isomer has the (1,4)-structure analogous to that of $[Re_7C(CO)_{21}Au(PPh_3)]^{2-}$; the other has one of the two remaining configurations. We assume the (1,2)-structure, since it has already been demonstrated that $[H_2Re_6C(CO)_{18}]^{2-}$ adopts this configuration [1]. At high temperatures (> 50°C), hydride scrambling over all the octahedral faces results in a fast equilibrium between the isomers and gives overall threefold symmetry. At temperatures below 10°C, the isomers are observed separately. If we assume local carbonyl scrambling on each isomer and hydride scrambling over all three (1,2)-faces of the (1,2)-isomer, both compounds are expected to show a 3/9/9 carbonyl pattern. The signals at δ

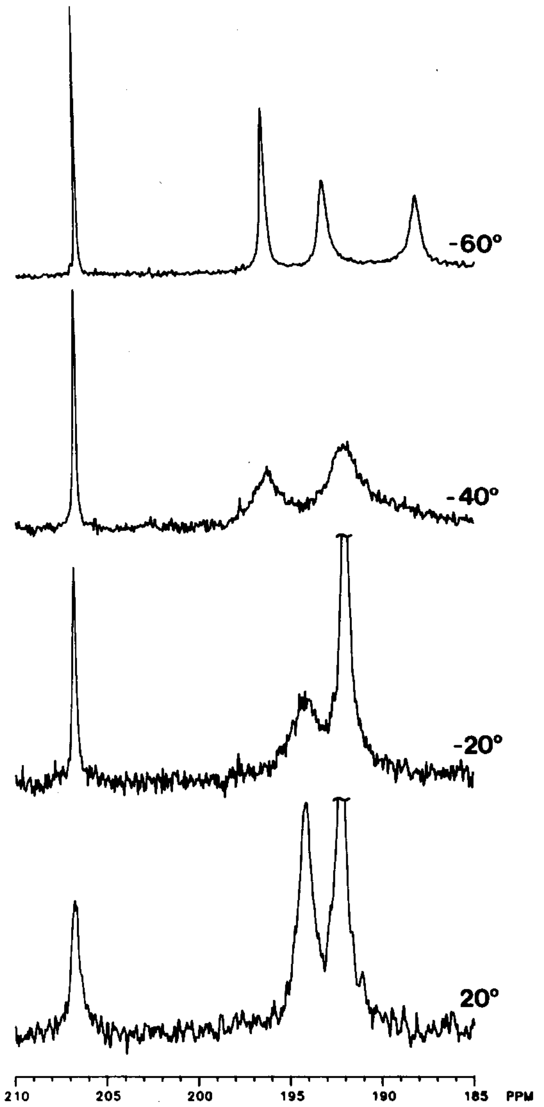

Fig. 2. Variable-temperature ^{13}C NMR spectra (carbonyl region) of $[PPN]_2[Re_7C(CO)_{21}Au(PPh_3)]$. Solvent: CD_2Cl_2.

192.3 and 191.7 are assigned to the (1,4)-isomer; those at δ 196.0 and 190.4 arise from the (1,2)-isomer. The resonance at δ 204.2 is due to overlapping signals from the capping Re carbonyls of both isomers; at temperatures below −20°C, a slight broadening in this peak is observed. At 0°C, the integrated intensities of the carbonyl resonances are consistent with a (1,4)/(1,2) ratio of 2/1. The intensities of the two hydride signals in the ^1H NMR spectrum integrate to the same ratio.

The low-temperature ^{13}C NMR spectrum of $[H_2Re_6C(\overset{*}{C}O)_{18}]^{2-}$ [1] was rationalized by assuming hindered local carbonyl scrambling of $Re(CO)_3$ units bonded to the bridging hydrogen atoms. If the same assumption is made here, an

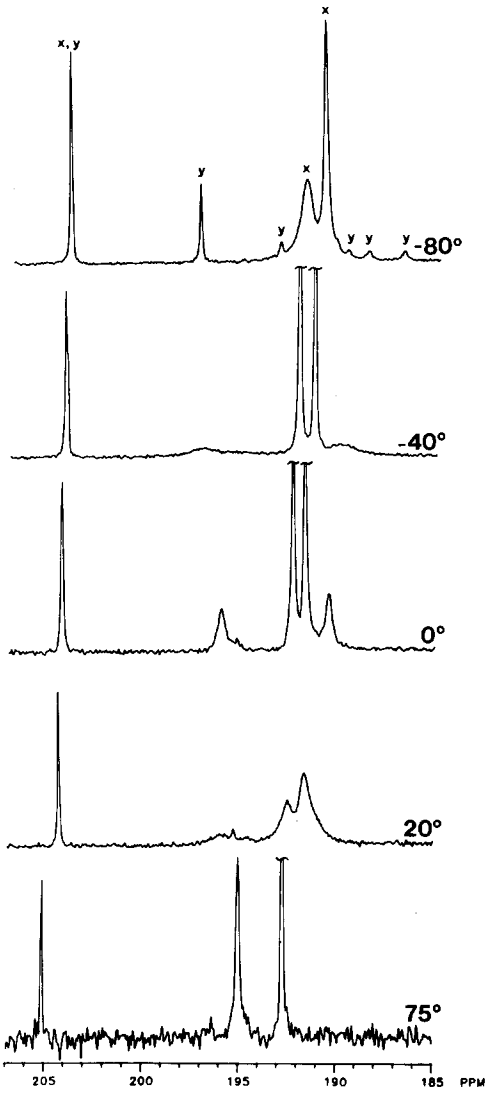

Fig. 3. Variable-temperature ^{13}C NMR spectra (carbonyl region) of $[PPN]_2[HRe_7C(CO)_{21}]$. Resonances arising from (1,4)-isomer indicated by (x); resonances arising from (1,2)-isomer indicated by (y). Solvent: CD_3NO_2 (75°C), CD_2Cl_2 (all other temperatures).

intermediate-exchange spectrum of the (1,2)-isomer, disregarding the capping Re carbonyls, would consist of a 6/3/2/2/2/2/1 pattern. Figure 5 illustrates the expected distribution of carbonyls adjacent to the (1,2) and (1,3)-faces of the (1,2)-isomer. The pattern arises from carbonyls f, f′, g, g′, h, h′ (6); a, b, b′ (3); c, c′ (2); d, d′ (2); e, e′ (2); j, j′ (2); and i (1). The -80°C spectrum of the $[HRe_7C(CO)_{21}]^{2-}$ mixture shows five peaks of relative intensity 6/3/2/2/2 (indicated by (y) in Fig. 3); we believe that the remaining signals are obscured by the (1,4)-isomer signals at δ 190.5–192.5. It is also evident that at this temperature the signals due to the (1,4)-isomer are beginning to broaden due to local exchange. A limiting low-temperature spectrum could not be obtained, even at -100°C.

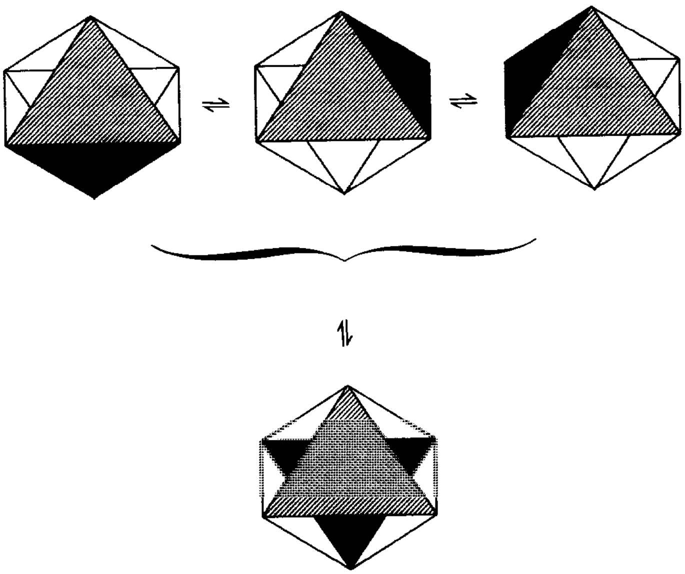

Fig. 4. Interconversion among the three possible (1,2) configurations (top) and the (1,4) configuration (bottom) of $[HRe_7C(CO)_{21}]^{2-}$. Shaded face represents the hydride cap; crosshatched face represents the $Re(CO)_3$ cap.

In conclusion, we have determined the solid-state structure of $[Re_7C(CO)_{21}Au(PPh_3)]^{2-}$ and have found it to adopt a (1,4)-bicapped octahedral geometry containing a μ_3-$Au(PPh_3)$ vertex. The variable-temperature ^{13}C NMR spectra of this complex are consistent with this structure as the sole species in solution, in agreement with previously reported ^{31}P NMR results [5]. However, the ^{13}C NMR spectra of $[HRe_7C(CO)_{21}]^{2-}$ show evidence for two distinct isomers in solution. The major isomer is again (1,4)-bicapped; the minor one is apparently (1,2)-bicapped. The (1,3)-isomer is not observed, but we suggest that it is a probable intermediate in both the degenerate scrambling among the (1,2)-isomers and the (1,2)/(1,4) interconversion. Despite the formal electronic analogy between H^+ and $Au(PPh_3)^+$ [9,12], the presence of two fluxional isomers of $[HRe_7C(CO)_{21}]^{2-}$ shows that the proton can be significantly more mobile over a cluster framework.

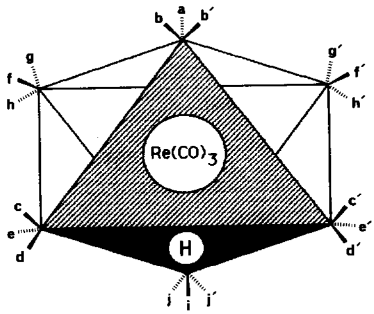

Fig. 5. Diagram representing the expected carbonyl disposition in the (1,2)-isomer of $[HRe_7C(CO)_{21}]^{2-}$.

Experimental

All reactions were carried out under nitrogen using standard Schlenk techniques. Solvents were dried and distilled immediately before use. $[PPN]_3[Re_7C(CO)_{21}]$ [4] and $Au(PPh_3)Cl$ [13] were prepared according to literature procedures. $HBF_4 \cdot OEt_2$ (Aldrich) was used as received. IR spectra were recorded on a Perkin–Elmer Model 281B spectrophotometer; ^1H and ^{13}C NMR spectra (360 and 90 MHz, respectively) were recorded on a Nicolet NT-360 instrument. Fast-atom bombardment mass spectra were obtained by the staff of the Mass Spectroscopy Center of the University of Illinois. Elemental analyses were performed by the Microanalytical Laboratory of the School of Chemical Sciences at the University of Illinois.

$[PPN]_2[Re_7C(CO)_{21}Au(PPh_3)]$

$[PPN]_3[Re_7C(CO)_{21}]$ (62.3 mg, 0.0177 mmol) and $Au(PPh_3)Cl$ (9.8 mg, 0.0198 mmol) were stirred in refluxing nitromethane for 30 min. The resulting solution was filtered, the solvent evaporated, and the residue dissolved in 5 ml of acetone. Addition of 40–50 ml of methanol followed by concentration and cooling gave red-brown crystals of product (39.9 mg, 66%). IR ν(CO) (acetone): 2039w, 1992vs, 1962w, 1932w, 1915w, 1877vw cm^{-1}. FAB-MS (neg. ion): m/z (^{187}Re) 2906 ($M-$ PPN), 2368 ($M-$ 2PPN), 2106 ($Re_7C(CO)_{21}Au$), $2106-28x$, $x = 1$–6 ($Re_7C(CO)_{21}Au - x$CO's). Anal. Found: C, 39.26; H, 2.41; N, 0.94; P, 4.68. $C_{112}H_{75}P_5N_2Re_7AuO_{21}$ calcd.: C, 39.11; H, 2.20; N, 0.81; P, 4.50%. The tetraphenylarsonium analogue was prepared by using $[Ph_4As]_3[Re_7C(CO)_{21}]$ as starting material; crystals suitable for X-ray diffraction studies were grown by slow diffusion of isopropanol into an acetone solution.

$[PPN]_2[HRe_7C(CO)_{21}]$

Cooled (−78°C) dichloromethane solutions of $[PPN]_3[Re_7C(CO)_{21}]$ (57.2 mg, 0.0163 mmol) and $HBF_4 \cdot OEt_2$ (3.0 μl, ca. 0.02 mmol) were combined and immediately gave a red-brown solution. This solution was reduced in volume under vacuum to 5 ml, and isopropanol (30–40 ml) was layered on top. Storage at −20°C for 3 d gave $[PPN]_2[HRe_7C(CO)_{21}]$ as a brick-red powder (21.4 mg, 44%). IR ν(CO) (acetone): 1998vs, 1982m sh, 1952vw, 1924w, 1887w cm^{-1}. ^1H NMR (CD_2Cl_2, 0°C): δ −19.27, −19.87 (both s, rel. ratio 2/1, hydrides of both isomers), 7.4–7.9 (m, PPN$^+$ protons). FAB-MS (neg. ion): m/z (^{187}Re) 2448 ($M-$ PPN), 1910 ($M-$ 2PPN), $1910-28x$, $x = 1$–8 ($HRe_7C(CO)_{21} - x$CO's). Anal. Found: C, 37.85; H, 2.12; N, 0.86. $C_{94}H_{61}P_4N_2Re_7O_{21}$ calcd.: C, 37.86; H, 2.06; N, 0.94%.

^{13}C-enriched samples of both compounds were prepared from $[PPN]_3[Re_7C(CO)_{21}]$ which had been synthesized from ca. 50% ^{13}CO enriched $Re_2(CO)_{10}$.

Crystal data

$C_{88}H_{45}As_2AuO_{21}PRe_7$, triclinic, $P\bar{1}$, a 12.553(2), b 14.446(3), c 25.181(5) Å, α 89.83(2), β 76.96(2), γ 86.78(2)°, V 4441.4(17) Å^3, $Z = 2$, D(calc) 2.34 g cm^{-3}, μ(Mo-K_α) 125.1 cm^{-1}, T 295 K. Nicolet R3 diffractometer, crystal deep red-brown (0.10 × 0.24 × 0.32 mm), 12,102 data collected ($4° \leq 2\theta \leq 48°$), 11,597 data unique and 9,085 observed, $F_0 \geq 2.5\sigma(F_0)$; $R_{(int)}$ 0.8%. The structure was solved by direct methods (SOLV) with considerable effort needed in finding a suitable starting set. An absorption correction based on Ψ-scan data was applied to the intensity data.

All non-hydrogen atoms with the exception of the carbon atoms in the phenyl rings were anisotropically refined. These rings were also constrained to rigid hexagons, d(C–C) 1.395 Å. Hydrogen atoms were treated as idealized, updated anisotropic contributions, d(C–H) 0.96 Å. At convergence, R_F 0.059, R_{wF} 0.062, and GOF 1.74. The highest peak in the final difference map, 1.8 e Å^{-3}, was within the Re_7 cluster and was followed by a rather noisy background in the 1.0–1.5 e Å^{-3} range (all within or near the Re_7 cluster). All computer programs in SHELXTL program library (Nicolet Corp.).

Acknowledgements

This work was supported at the University of Illinois by National Science Foundatioin grants DMR 83-16981 to the Materials Research Laboratory and CHE 84-07233 to J.R.S. FAB-mass spectra were obtained with instrumentation supported in part by a grant from the National Institutes of Health (GM 27029).

References

1 G. Ciani, G. D'Alfonso, M. Freni, P. Romiti, and A. Sironi, J. Organomet. Chem., 244 (1983) C27.
2 G. Ciani, G. D'Alfonso, M. Freni, P. Romiti, and A. Sironi, J. Chem. Soc., Chem. Commun., (1982) 339.
3 G. Ciani, G. D'Alfonso, M. Freni, P. Romiti, and A. Sironi, J. Chem. Soc., Chem. Commun., (1982) 705.
4 C.M.T. Hayward and J.R. Shapley, Inorg. Chem., 21 (1982) 3816.
5 T. Beringhelli, G. D'Alfonso, M. Freni, G. Ciani, and A. Sironi, J. Organomet. Chem., 295 (1985) C7.
6 B.F.G. Johnson, J. Lewis, W.J.H. Nelson, J. Puga, P.R. Raithby, D. Braga, M. McPartlin, and W. Clegg, J. Organomet. Chem., 243 (1983) C13.
7 C.F. Barrientos-Penna, F.W.B. Einstein, T. Jones, and D. Sutton, Inorg. Chem., 24 (1985) 632.
8 P.D. Doyle, B.J. Johnson, A. Buehler, and L.H. Pignolet, Inorg. Chem., 25 (1986) 5.
9 J.W. Lauher and K. Wald, J. Am. Chem. Soc., 103 (1981) 7648.
10 T.L. Blundell and H.M. Powell, J. Chem. Soc. A, (1971) 1685.
11 C.M.T. Hayward, Ph.D. Thesis, University of Illinois, Urbana, 1984.
12 K.P. Hall and D.M.P. Mingos, Prog. Inorg. Chem., 32 (1984) 237.
13 C. Kowala and J.M. Swan, Aust. J. Chem., 19 (1966) 547.